frontiers | Frontiers in Energy Research

TYPE Original Research
PUBLISHED 31 October 2024
DOI 10.3389/fenrg.2024.1466165

OPEN ACCESS

EDITED BY
Hugo Morais,
University of Lisbon, Portugal

REVIEWED BY
Prakash Chandra Sahu,
Veer Surendra Sai University of Technology, India
Naladi Ram Babu,
Aditya Engineering College, India

*CORRESPONDENCE
A. S. Veerendra,
veerendra.babu@manipal.edu
Kothalanka K. Pavan Kumar,
kothalanka_rs@ee.nits.ac.in
Rahmat Ullah,
ullahr1@cardiff.ac.uk

RECEIVED 17 July 2024
ACCEPTED 14 October 2024
PUBLISHED 31 October 2024

CITATION
Kumar KKP, Das DC, Soren N, Veerendra AS, Flah A, Alkuhayli A and Ullah R (2024) A multi-energy inertia-based coordinated voltage and frequency regulation in isolated hybrid power system using PI-TISMC. *Front. Energy Res.* 12:1466165. doi: 10.3389/fenrg.2024.1466165

A multi-energy inertia-based coordinated voltage and frequency regulation in isolated hybrid power system using PI-TISMC

Kothalanka K. Pavan Kumar[1]*, Dulal Chandra Das[1], Nirmala Soren[2], A. S. Veerendra[3]*, Aymen Flah[4,5,6,7], Abdulaziz Alkuhayli[8] and Rahmat Ullah[9]*

[1]Department of Electrical Engineering, NIT Silchar, Silchar, India, [2]Department of Electrical Engineering, BIT Sindri, Sindri, India, [3]Department of Electrical and Electronics Engineering, Manipal Institute of Technology, Manipal Academy of Higher Education, Manipal, India, [4]Processes, Energy, Environment and Electrical Systems (Code: LR18ES34), National Engineering School of Gabès, University of Gabès, Gabès, Tunisia, [5]MEU Research Unit, Middle East University, Amman, Jordan, [6]The Private Higher School of Applied Sciences and Technology of Gabes (ESSAT), University of Gabes, Gabes, Tunisia, [7]Applied Science Research Center, Applied Science Private University, Amman, Jordan, [8]Electrical Engineering Department, College of Engineering, King Saud University, Riyadh, Saudi Arabia, [9]Advanced High Voltage Engineering Research Centre, Cardiff University, Cardiff, United Kingdom

This paper proposes novel multi-energy inertia support for simultaneous frequency and voltage control of an isolated hybrid power system (IHPS). Multi-energy storage (gas inertia – hydrogen storage, thermal inertia – solar thermal storage, hydro inertia – gravity hydro storage, chemical inertia – battery energy storage) supported by demand side management (DSM) for simultaneous voltage and frequency regulation and backed by biodiesel generators, are the essential elements of IHPS. A novel control strategy of concurrent virtual droop control, virtual damping control, virtual inertia control, and virtual negative inertia control is proposed to utilise multiple inertia sources and to improve LFC and AVR performance effectively. The effective coordination of inertia sources in eradicating oscillations in IHPS, is aided by a developed cascaded proportional integral-tilt-integral-sliding mode (PI-TISMC) controller. The performance of PI-TISMC is compared with PID, PI-PID, and PI-SMC controllers. A maiden attempt has been done by training five diverse classes of optimization techniques to optimize the parameters of controllers in the present work. The results are evaluated in MATLAB and it is evident from the results that the performance of frequency control is improved by 6.5%, 7.8% and 3.4 s (over shoot, undershoot, and settling time). The performance of frequency control is improved by 6.5%, 7.8% and 3.4 s (over shoot, undershoot, and settling time). Similarly, the performance of voltage control is improved by 6.7%, 4.8% and 2.3 s (over shoot, undershoot, and settling time) by employing developed PI-TISMC controller and proposed concurrent inertia control. The combination exhibits superior

performance in minimizing oscillations in IHPS due to variations in loading and solar insolation.

KEYWORDS

cascaded SMC, demand side management, isolated hybrid power systems, optimization techniques, simultaneous frequency and voltage control, virtual inertia

1 Introduction

1.1 Motivation

An isolated hybrid power system generates the required power to satisfy the required load from various remote and renewable sources as the system is not connected to the primary grid. Renewable sources (RES), such as PV, wind, biomass etc., provides the power essential for IHPS, backed by energy storage sources (ESS), depending on their availability and shortage. Frequency and voltage deviations will be regular in these types of systems due to the volatile nature of the environment and load. These oscillations are primarily addressed by the inertia of the rotating machines available at the source end, which are low in portion in IHPS, as shown in Figure 1A. Recently, the shortage of inertia has been addressed by virtual inertia provided by ESS. The effective utilization of available ESS for IHPS can address frequency and voltage oscillations. The inertia control alone couldn't suppress these oscillations, which requires appropriate secondary control mechanism, as shown in Figure 1B.

This led to a resourceful research contribution towards secondary controllers aiding virtual inertia control to support stability of the IHPS. The following section provides such glimpses of authors contribution towards stability issues of modern power systems.

1.2 Literature survey

Reports (Denholm et al., 2020) at NREL state that integrating renewable sources into the traditional grid and remote areas is progressing rapidly. These integration RES reduces system inertia, which leads to contingencies, as shown in Figure 1B. International practices of inertia estimation and offline estimation methods in India are assessed by authors in Report on Assessment of Inertia in Indian Power System (2022), and a detailed analysis of the inertia-generating units in India implies load-side inertia contribution, estimated to be 20% of total system inertia. Khan et al. (2023) address frequency stability challenges in hybrid power systems, exploring load frequency control methodologies and power system flexibility and highlighting the need for fine-tuned controllers and virtual inertia backup. A virtual gas inertia model (Miao et al., 2023a) that represents the gas storage's capability to mitigate power impact and explores the joint use of gas inertia with other energy forms, focusing on fully utilizing multi-energy inertia resources like thermal and natural gas energy inertia to power support optimization. The potential of gas-thermal inertia-based frequency response strategy in Integrated Energy Systems (IESs) (Miao et al., 2023b), leveraging the slow-dynamic characteristics of gas-thermal systems, addresses power grid inertia challenges. The limitations of single control methods are overcome by proposing an integrated control method that combines virtual inertia control, virtual negative inertia control, and virtual droop control, thereby improving comprehensive control performance for PFR (Zhu et al., 2021). This integrated approach enhances the frequency regulation effect but also helps in reducing the ESS capacity requirements, making the system more efficient and cost-effective for frequency regulation applications. Thus, the combined multi energy inertia support is an emerging research area for addressing stability enhancement of hybrid power systems.

Ranjan et al. (2021) discuss voltage and frequency control in a 3-area interconnected hybrid power system with solar and wind power, incorporating FACTS devices and a demand response scheme. Latif et al. (2023) developed a frequency-voltage response model for a photon exchange membrane fuel cell (PEMFC) for the first time. They assessed the dynamic responses using an integer order proportional-integral-derivative (IOPID) controller. A novel approach is introduced in Kumar Barik et al. (2019) focusing on optimal load-frequency regulation of 4-interconnected unequal hybrid microgrids with demand response support. The paper utilizes particle swarm optimization (PSO) tuning classical PID controllers for load-frequency control of bio-renewable cogeneration-based interconnected hybrid microgrids with demand response support, ensuring efficient power management in different climatic scenarios. The efficacy of the cascaded PI-TID controller tuned using chaotic butterfly optimization algorithm (CBOA) (Bhuyan et al., 2023) through sensitivity analysis under significant changes in source and load conditions, highlighting its robustness and adaptability. Analysis of dynamic performance of the hybrid generation system using time-domain simulations under various operating conditions and disturbances, presenting optimal gain settings for classical and PSO-based PI controllers (Das et al., 2011). Most of the single and multi-area power systems are addressed by the authors for load side control along with sources side control. The authors contribution towards research on load side control like DSM for virtual inertia supported IHPS is very few.

A robust load-frequency controller for the dynamic stability of interconnected power systems was proposed in Yang and Lu (1999), Vrdoljak et al. (2009). Mi et al. (2013), Xinxin et al. (2020), and Kumar et al. (2021) proposed decentralised sliding mode (SM) LFC designed for multi-area interconnected power systems with robust stability. The proposed method outperforms other reported methods in frequency deviation improvement. PI switching surface is considered in the above works, and Lyapunov stability theory proof is studied for controller stability studies. FOSMC enhance system stability and outperforms PID, FOPID, and SMC (Guha et al., 2021). FOSMC effectively dampens power-frequency oscillations in low-inertia systems. Pavan Kumar et al. (2024) introduced the TISMC technique with proven stability

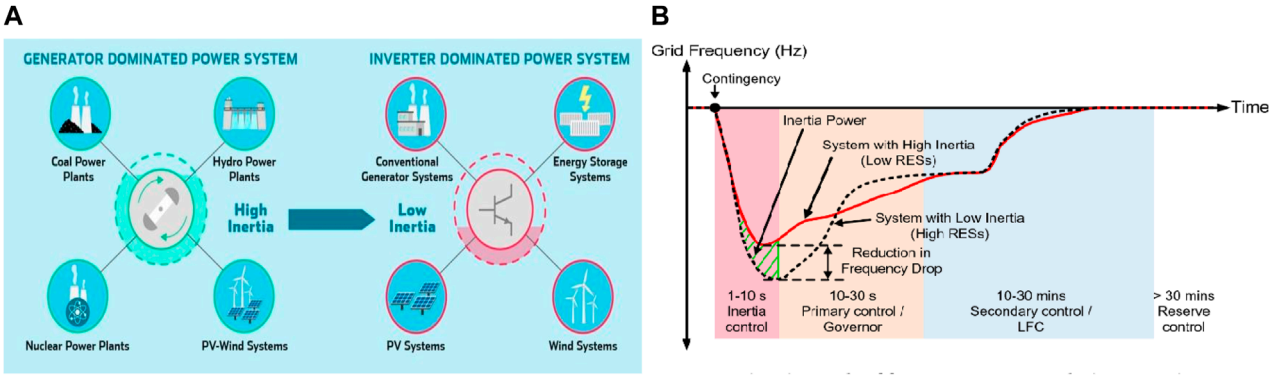

FIGURE 1
(A): Inertia support in generating sources. **(B)**: Control scheme of frequency disturbance.

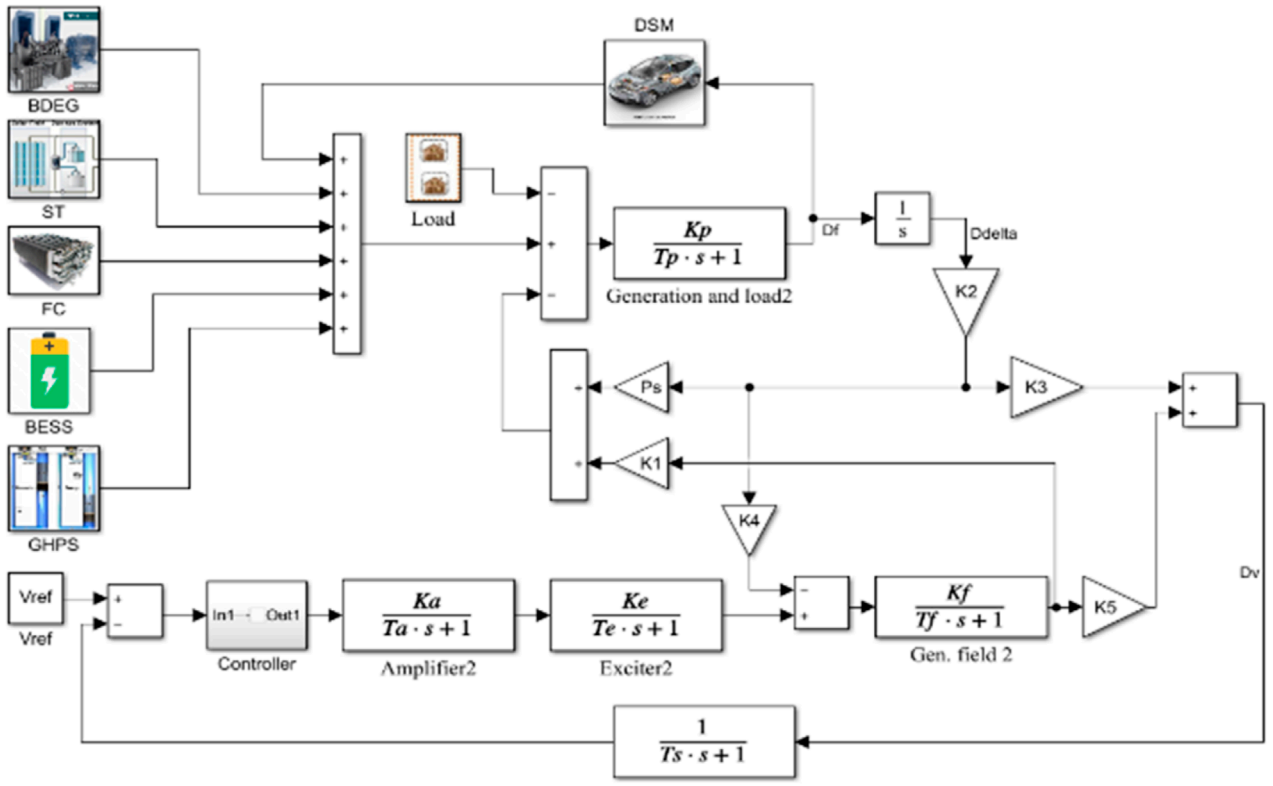

FIGURE 2
Proposed IHPS.

and improved AVOA for optimising controller parameters for mitigating frequency fluctuations. A comparative analysis of cascaded SMC and FOSMC for ball trajectory control (Das and Roy, 2016; Roy et al., 2018) shows that the fractional order SMC (FOSMC) outperforms SMC in speed and tracking accuracy. Contribution towards design of controllers for frequency enhance of micro grid performance utilizing fuzzy logic (Chandra Sahu et al., 2023; Kumar Mohapatra et al., 2024) and in cascaded fuzzy logic connection (Kumar Mohapatra et al., 2024). Considering the advantages from literatures behind cascading controllers to enhance their stability and to improve their performance is a futuristic work. Cascading nonlinear controllers like SMC have been identified as less focused area in terms of addressing stability issues related to modern power systems.

1.3 Contribution

The paper introduces the following novel contributions from the detailed literature survey.

- Developed a novel multi-energy inertia-based power support approach (gas inertia – hydrogen storage, thermal inertia – solar thermal storage, hydro inertia – gravity hydro storage, chemical inertia – battery energy storage) for simultaneous voltage and frequency regulation.
- Proposed a novel control strategy considering concurrent virtual droop control, virtual damping control, virtual inertia control, and virtual negative inertia control to improve LFC and AVR performance.
- Implemented DSM (controllable load - hybrid electric vehicle) strategy in an isolated hybrid power system for simultaneous voltage and frequency regulation.
- Developed a novel cascaded PI-TISMC and to inspect its performance with PID, PI-PID, and PI-SMC controllers.
- A comparative assessment of five different classes (evolutionary, swarm-based, physics-based, human-inspired, bio-inspired) of optimization strategies in controlling voltage and frequency oscillations with rigorous simulation studies.
- Validated the dynamic stability of a single area isolated hybrid power system subject to change in loading and solar insolation using MATLAB simulation.

2 Modelling of the isolated power system

The present work considers an isolated hybrid power system, as Figure 2 shows. A solar-powered parabolic trough collector system of 1 Mwe with thermal storage for 8 h back up and a biodiesel generator system of 200 KW meets the required load demand. These power sources are backed by ESS–aqua electrolyser-powered fuel cells of 50 KW, gravity hydro energy storage of 50 KW, and battery energy storage systems of 20 KW. Equation 1 provides active power

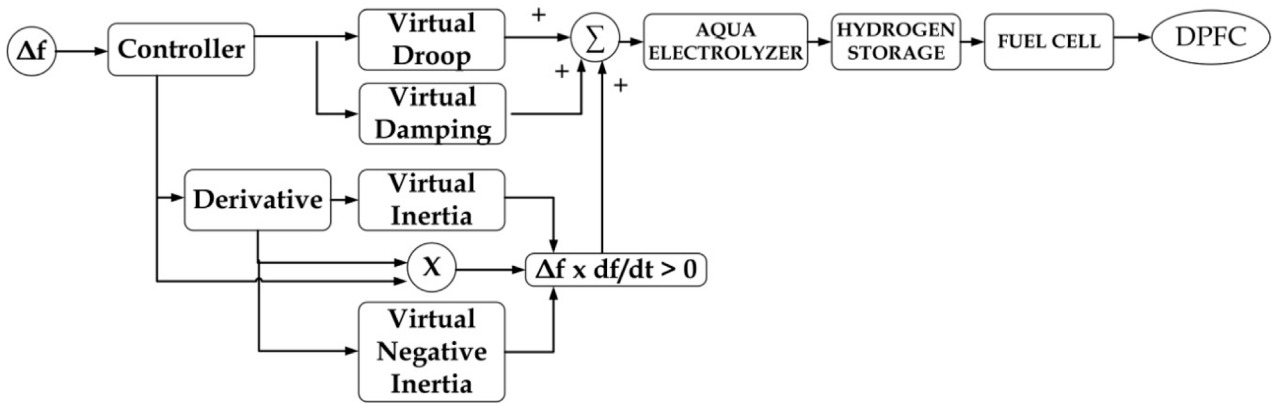

FIGURE 3
Virtual gas inertia system.

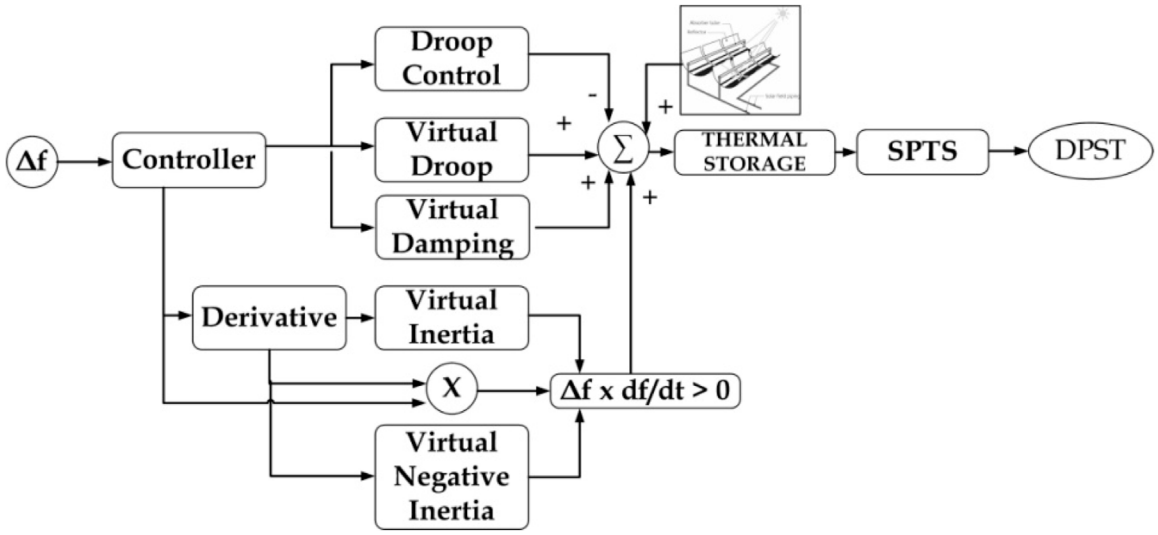

FIGURE 4
Virtual thermal inertia system.

generation (P_T) for all the sources of IHPS.

$$P_T = P_{ST} \pm P_{FC} + P_{BDEG} \pm P_{BESS} \pm P_{GHPs} \pm P_{HEV} - P_{L1} \quad (1)$$

2.1 Modelling of bio-diesel generator

Biodiesel extracted from the transesterification of waste edible oils/suitable energy crops has properties analogous to diesel (Denholm et al., 2020). The linearized model of BDEG is expressed as in Equation 2, considering the actions of the inlet valve and engine.

$$TF_{BDEG} = \left(\frac{K_{be}}{1 + sT_{be}}\right)\left(\frac{K_{ba}}{1 + sT_{ba}}\right) \quad (2)$$

2.2 Multi-energy inertia approach

Inertia support is highly necessary for the power system to enhance stability. It's a regular practice for synchronous generators to take part in inertia support. In the RES integrated power system, the lack of rotating machines results in less inertia support (Tamrakar, 2017). Hence, virtual inertia is introduced with multiple storage devices to enhance the stability of the system. In Miao et al. (2023a), detailed virtual inertia support for the stability of the power system is discussed. Multi-energy inertia support for the power system is a new concept detailed in Miao et al. (2023b). From this idea, in the present work, we proposed a concurrent multi-energy inertia system for voltage and frequency support of IHPS. Concurrent virtual damping, virtual droop, virtual inertia and virtual

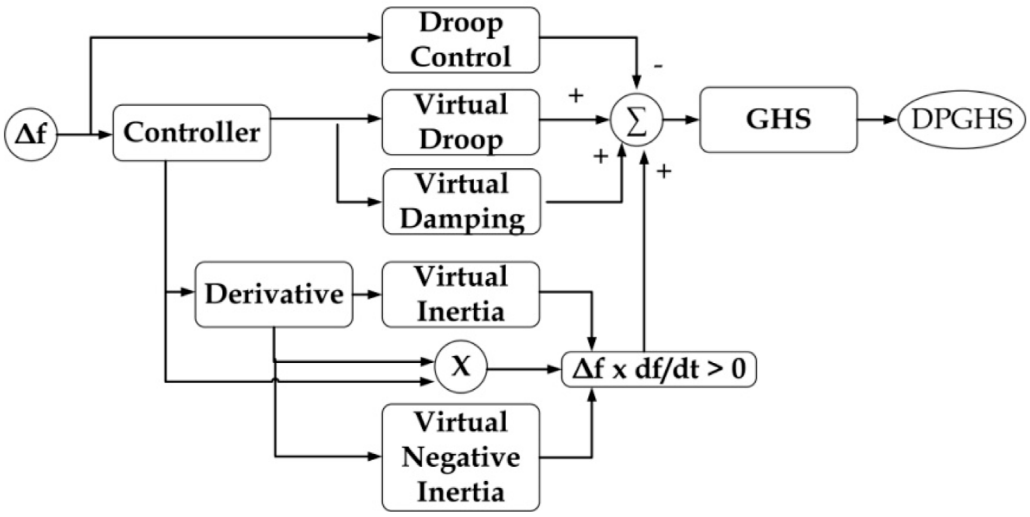

FIGURE 5
Virtual hydro inertia system.

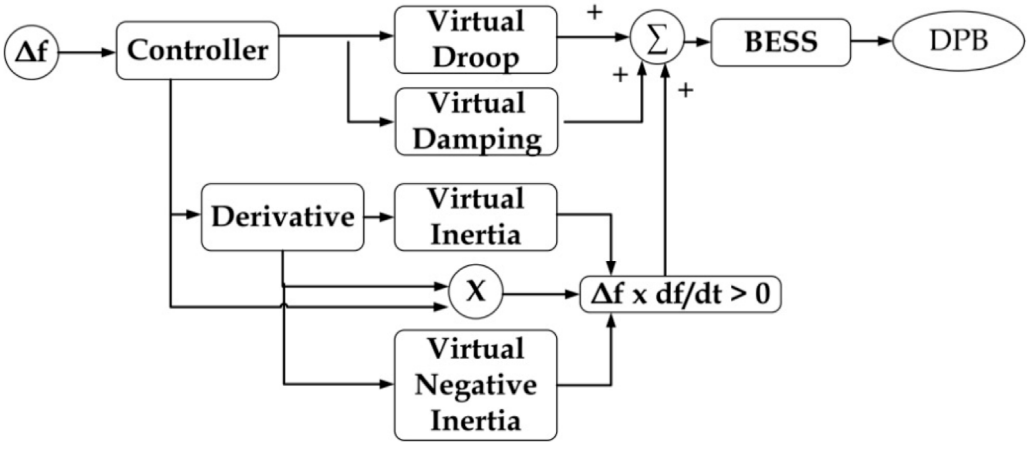

FIGURE 6
Virtual chemical inertia system.

negative inertia techniques are proposed in the present work, as discussed below.

2.3 Virtual damping control

In IHPS, virtual damping control plays a vital role in time-based control of oscillation caused by a mismatch in frequency/voltage. The damping signal is generated by the proportional gain of the error signal as given in Equation 3.

$$\Delta P_D = K_D \times \Delta f \tag{3}$$

2.4 Virtual droop control

The virtual droop control regulates the active power output of an Energy Storage System (ESS) based on the system's droop characteristic and frequency deviation. By utilizing virtual droop control, the steady-state frequency deviation of the system can be minimized. The virtual droop control mechanism determines the active power output of ESS as given in Equation 4.

$$\Delta P_{DP} = -K_D \times \Delta f \tag{4}$$

2.5 Virtual inertia control

Under virtual inertia control, the Energy Storage System (ESS) replicates the inertia properties typically seen in a synchronous machine. The charging or discharging capability of the ESS is directly influenced by the rate of change in frequency, serving to alleviate fluctuations in system frequency and bolster overall system stability. The functionalities of the ESS can be delineated as follows as given in Equation 5:

$$\Delta P_{I1} = -K_I \times d(\Delta f)\, dt \tag{5}$$

2.6 Virtual negative inertia control

Virtual inertia control is effective in reducing system frequency deviations, but it may impede frequency recovery. Therefore, virtual negative inertia control can be implemented during the recovery phase to accelerate the process. The performance of Energy Storage Systems (ESS) under virtual negative inertia control is presented below in Equation 6 as follows:

$$\Delta P_{I2} = K_I' \times d(\Delta f)\, dt \tag{6}$$

This paper presents a comprehensive control approach that utilises frequency deviation and rate of change of frequency deviation. The integrated control strategy incorporates virtual damping control, virtual droop control, virtual inertia control, and virtual negative control to improve the frequency regulation effect. The frequency regulation processes can be divided into two phases: frequency deterioration and frequency recovery, as shown in Figure 1B. During the frequency deterioration phase, the system frequency moves away from the nominal frequency, with the criteria defined as ($\Delta f * df/dt > 0$). In the frequency recovery phase, the system frequency moves back towards the nominal frequency, with the criteria defined as ($\Delta f * df/dt < 0$). The proposed integrated control strategy integrates virtual damping, virtual droop control and virtual inertia control during the frequency deterioration phase to lessen frequency deviation and prevent frequency deterioration. In the frequency recovery phase, virtual damping, virtual droop control and virtual negative inertia control are combined to reduce frequency deviation and hasten frequency recovery. The ESS output power in the frequency regulation phase can be expressed as:

$$\Delta P_{PFR} = \begin{cases} \Delta P_D + \Delta P_{DP} + \Delta P_{I1}, if \Delta f \times (df/dt) > 0 \\ \Delta P_D + \Delta P_{DP} + \Delta P_{I2}, if \Delta f \times (df/dt) < 0 \end{cases} \tag{7}$$

2.7 Gas inertia – Hydrogen storage

An aqua electrolyser-powered fuel cell with hydrogen storage is considered to provide gas inertia support to the IHPS. Gas inertia is modelled to mitigate power fluctuations in isolated power systems. Gas network constraints are analysed for the system's strategy, economy, and power outputs (Zhou et al., 2024a; Zhou et al., 2024b).

The proposed concurrent virtual inertia strategy of the hydrogen gas storage system is presented in Figure 3.

2.8 Thermal inertia – Solar thermal storage

Solar-powered parabolic trough collector system is the main source of power generation in IHPS. Solar power generating system are backed with thermal storage to provide power without required insolation. Thermal storage provides the concurrent virtual inertia strategy, as shown in Figure 4.

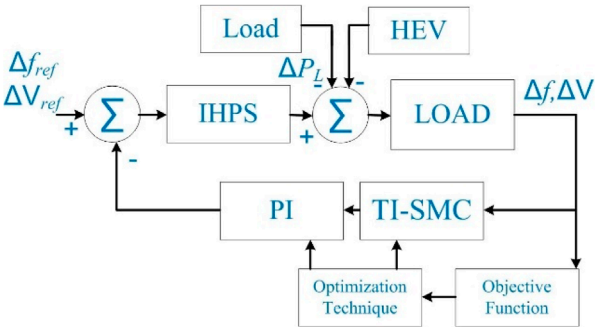

FIGURE 7
Proposed control scheme for IHPS.

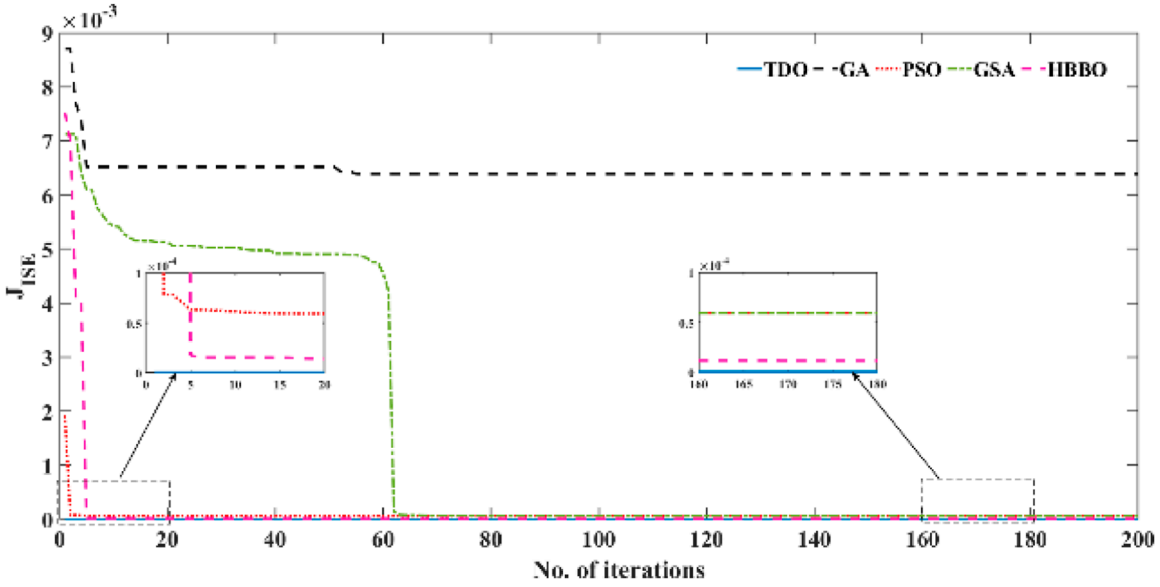

FIGURE 8
Convergence curvers of Optimization Techniques.

TABLE 1 Comparison of optimization techniques.

	Avg.	Std. Dev	Median
GA	5.06E-07	3.03E-08	4.87988E-07
PSO	6.89E-05	0.000131	1.16443E-05
GSA	0.000125	0.00026	5.92468E-05
HBBO	0.001623	0.000827	6.07201E-05
TDO	0.006453	0.002383	0.006386761

2.9 Hydro inertia – Gravity hydro storage

Hydro storage is a vital option for high-rated storage capacity. The working principle of GHPS is explained in Berrada et al. (2027), Yaghoubi et al. (2024), and detailed modelling for solar-powered energy systems is provided. In the present work, a concurrent virtual inertia model of GHPS is proposed and implemented for simultaneous frequency and voltage control of IHPS, as shown in Figure 5.

2.10 Chemical inertia – Battery energy storage

BESS is a highly used ESS option because of their longer life and cost (Meng et al., 2024a; Meng et al., 2024b). In the present work, a concurrent virtual inertia model of a BESS is proposed and implemented for simultaneous frequency and voltage control of IHPS, as shown in Figure 6.

2.11 Demand side management – Hybrid electric vehicle

HEV is a controllable load considered in the present work. Load side control provides a lesser impact on the system than the source side control (Kumar Barik et al., 2019).

$$\Delta P_{HEV} = \begin{cases} -\dfrac{\Delta f}{|\Delta f_m|}\Delta P_{DSM} \; ; if - \Delta f_m \le \Delta f \le \Delta f_m \\ -\dfrac{\Delta f}{|\Delta f|}\Delta P_{DSM}; otherwise \end{cases}$$

$$TF_{HEV} = \frac{K_{HEV}}{1 + sT_{HEV}};$$

$$\Delta P_{DSM} = \Delta P_{SOC} * TF_{HEV}$$

3 Proposed methodology

3.1 Objective function

The main objective in the present work is to minimise voltage and frequency oscillation by properly tuning controllers using optimisation techniques. The objective function is formed by the algebraic relation of error signals in the system, and optimization techniques are implemented to minimize the function, as shown in Figure 2. In the present work, integral square error (J_{ISE}) is considered an objective function as presented in Equation 7.

$$J_{ISE} = \int_0^T (|\Delta f^2 + \Delta v^2|)dt$$

3.2 Modelling of the controller

In contemporary times, the sliding mode controller (SMC) has gained recognition as a reliable, robust controller that can be applied to linear and non-linear systems. Given the dynamic fluctuations in solar insolation and load over time, this controller is particularly well-suited for the current issue. Introducing the cascaded PI- TISMC, with a tilt integral order sliding surface, represents an innovative approach, offering the controller additional flexibility to minimise frequency and voltage deviations promptly as shown in Figure 7.

3.2.1 Cascaded PI-TISMC controller

Our previous work (Pavan Kumar et al., 2024) established the various advantages of the TISMC controller, and its detailed modelling was considered. The development of the sliding mode surface and the control law together fulfil the complete design of the SMC controller. In the present work PI controller is cascaded with TISMC to enhance the system's stability and reduce chattering effect. A decentralized control scheme of SMC is considered in the work for multiple energy inertia sources (Zhang H. et al., 2023; Li et al., 2022). The state space representation of an IHPS is presented in Equation 8, with various states of the state space model of the IHPS outlined in Equations 9–14. External disturbances such as the fluctuations in load (P_L) and insolation (I) are considered, while the cascaded PI-TISMC output is utilised as the control input for the IHPS (Tian et al., 2024; Wang et al., 2024).

$$\dot{x}(t) = Ax(t) + Bu(t) + FB_d(t) + GH(t) \tag{8}$$

A, B, F, J, G ($\in$ R) are system matrices.
x(t) is the system state matrix.
u(t) is control matrix.$B_d(t)$ is the disturbance matrix.

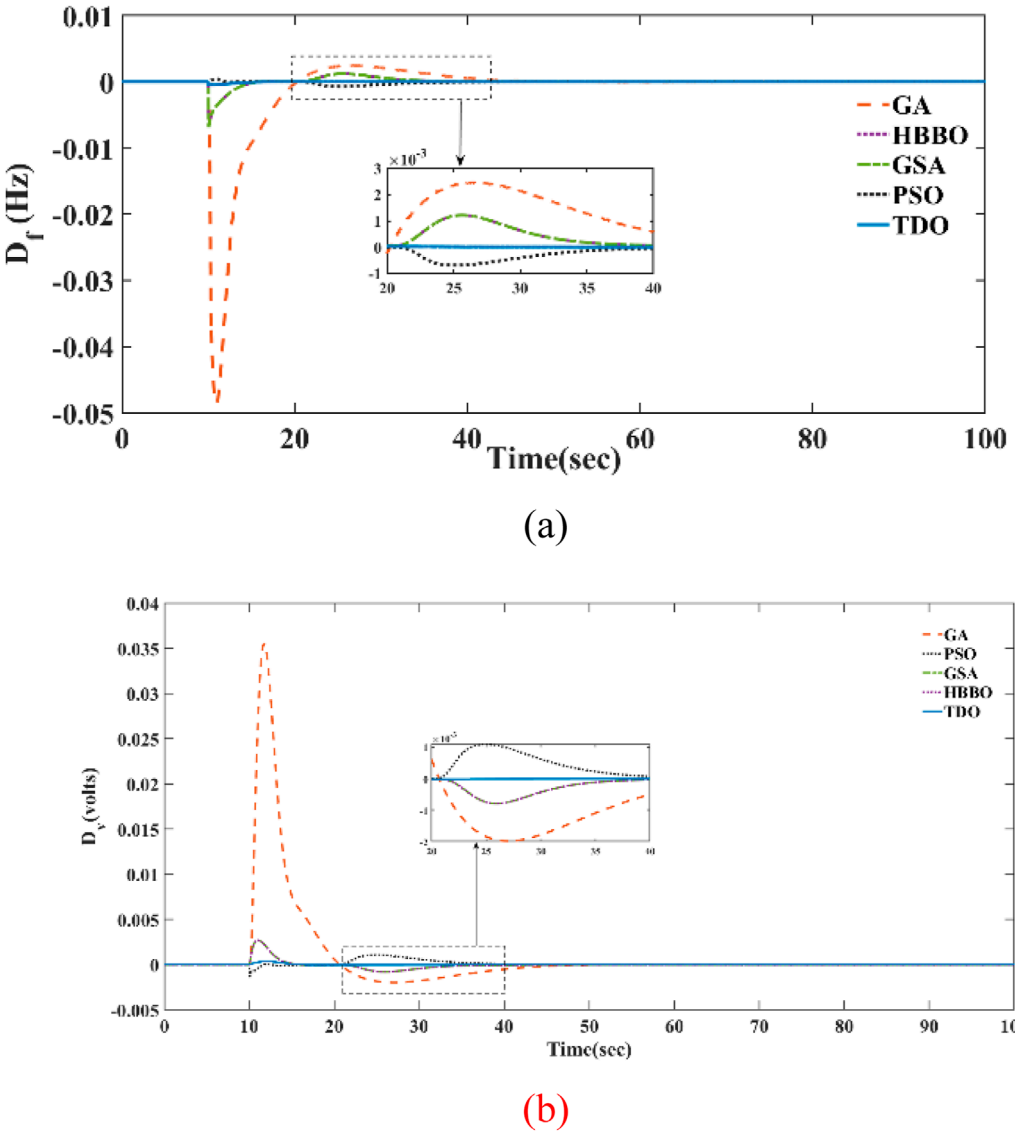

FIGURE 9
Comparison of Optimization Techniques of **(A)** frequency and **(B)** voltage deviations.

H(t) is the state matrix of other control areas.

SMC - 1

$$x_{11}(t) = \left[\Delta f \Delta P_{bg} \Delta X_{bg}\right]^T \tag{9}$$

SMC - 2

$$x_{12}(t) = \left[\Delta f \Delta P_s \Delta T_p \Delta P_m \Delta X_c \Delta T_h \Delta P_{sc}\right]^T \tag{10}$$

SMC - 3

$$x_{13}(t) = \left[\Delta f \Delta P_g \Delta X_{gh} \Delta X_{ga'}\right]^T \tag{11}$$

SMC - 4

$$x_{14}(t) = \left[\Delta f \Delta P_{b'}\right]^T \tag{12}$$

SMC - 5

$$x_{15}(t) = \left[\Delta f \Delta P_h \Delta X_{gc} \Delta X_{gg'}\right]^T \tag{13}$$

SMC - 6

$$x_{16}(t) = \left[\Delta X_f \Delta X_e \Delta X_a \Delta X_s \Delta \delta_2\right]^T \tag{14}$$

Considering above state equations and data from Equation 8, the stability and superiority of the proposed controller is proved. The PI-TISMC controller considered in the work is a decentralized controller, SMC-1 to SMC -6, addressing BDEG, ST, FC, BESS, GHPS, and voltage control, respectively (Jiao et al., 2024; Zhang et al., 2024).

3.3 Choice of optimization function

In the present paper five optimization techniques, that works on five different principles are considered as follows:

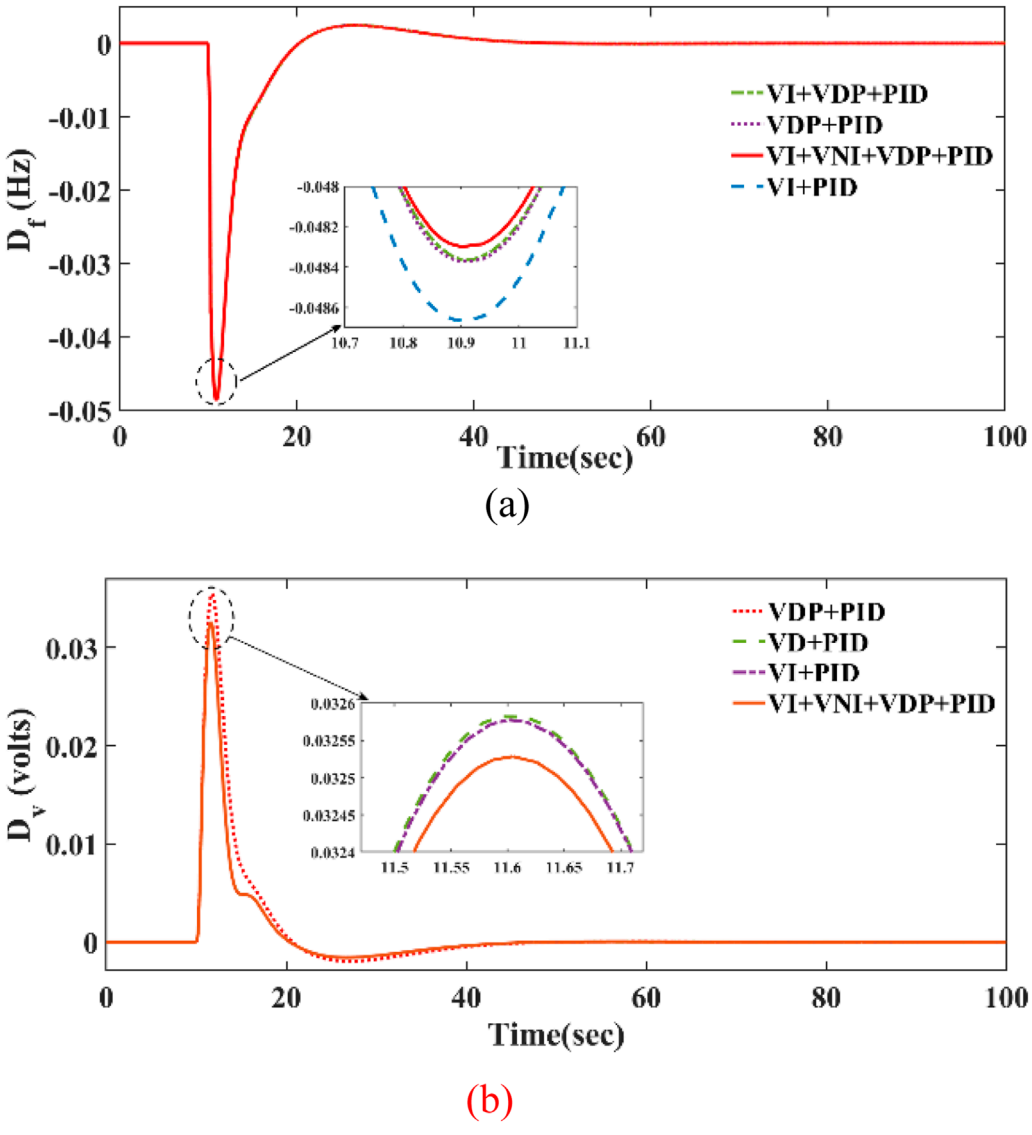

FIGURE 10
Comparison of virtual inertia techniques of **(A)** frequency and **(B)** voltage deviations.

1. Genetic algorithm (evolutionary principle based) Das et al., 2012,
2. Particle swarm optimization (swarm based) Das et al., 2011,
3. Gravitational search algorithm (physics based) Ghosh et al., 2021,
4. Human behaviour-based algorithm (human inspired) Ahmadi, 2017,
5. Tasmanian devil optimization (bio-stimulated based) Dehghani et al., 2022

These different optimization techniques are implemented for frequency and voltage oscillations individually. But comparison of these class of techniques for concurrent voltage and frequency control is a notable novel attempt (Zhang J. et al., 2023; Ma et al., 2019; Shirkhani et al., 2023).

4 Simulation results

Under multiple scenario's the proposed controller and virtual inertia technique has been verified for the IHPS system considered in the work.

4.1 Selection of optimization techniques

In the initial phase an efficient optimization technique has been chosen for controller parameter tuning. The results have been analysed for step increment in disturbance of load and solar insolation of microgrid system. Optimization techniques were used to tune PID controller parameters for the system. Five different classes of optimization techniques have been considered for the

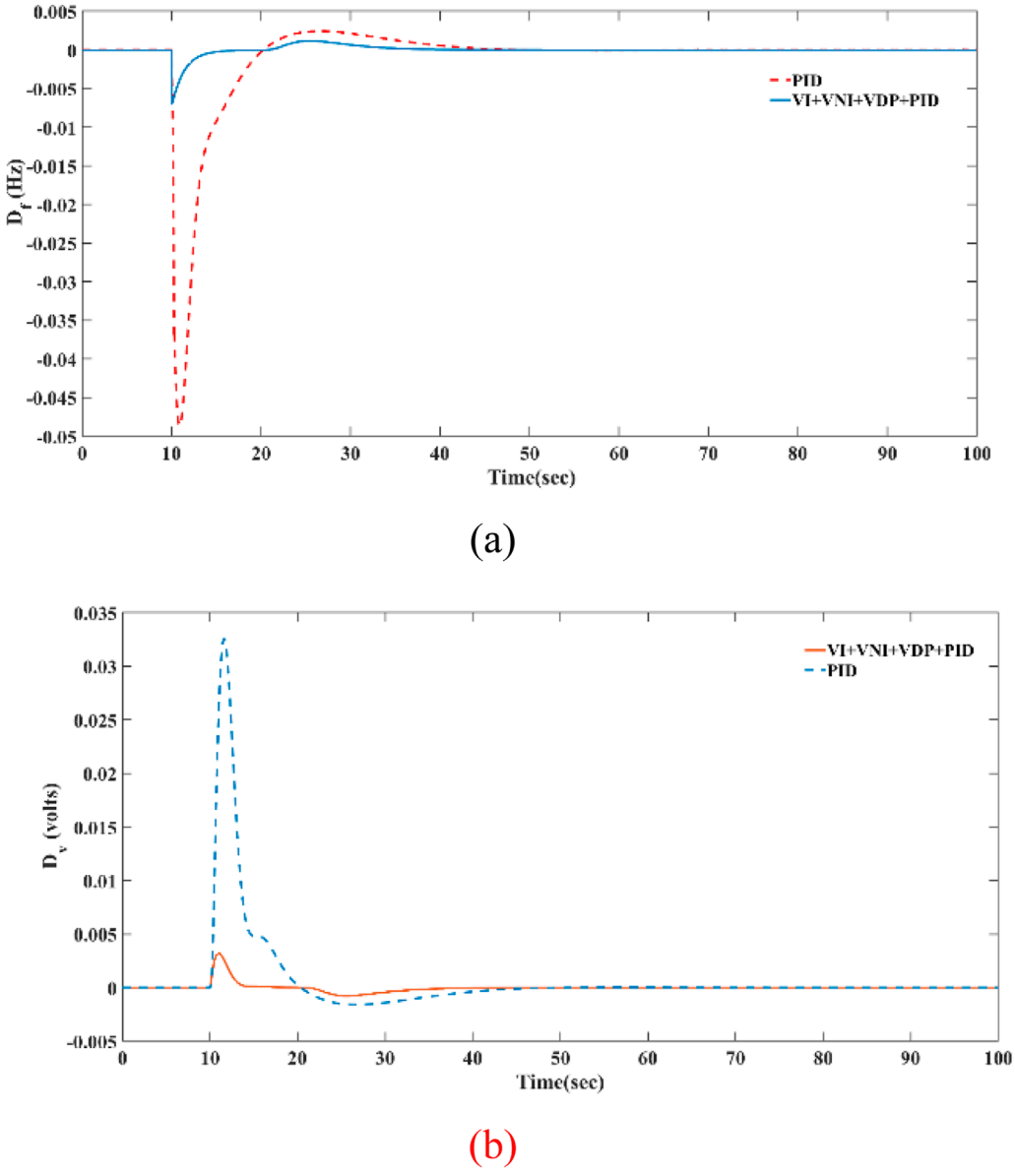

FIGURE 11
Comparison of PID controller performance with and without virtual inertia techniques for **(A)** Frequency control, **(B)** Voltage control.

work, genetic algorithm (GA- evolutionary based), particle swarm optimization (PSO-swarm based), gravitational search algorithm (GSA-physics based), human behaviour-based optimization (HBBO- human behaviour based), Tasmanian devil optimization (TDO-bio inspired). The performance comparison of optimization techniques is presented below (Ju et al., 2022; Wang et al., 2023; Liu et al., 2024).

Convergence curves of multiple optimization techniques considered in the work are shown in Figure 8 and compared in Table 1. The results of frequency and voltage deviation for multiple optimization techniques are presented in Figure 9.

It is evident from the results that TDO (bio-inspired) algorithm exhibits minimum deviations and fastest settling time for disturbances, supporting its better performance compared to other classes of techniques. So, for the rest of analysis TDO is considered for tuning controller parameter.

4.2 Comparison of virtual inertia techniques

The proposed concurrent virtual inertia techniques are compared with each individual combination to opt the best technique from it. The results have been analysed for step increment in disturbance of load and solar insolation of microgrid system and presented in Figure 10.

It is evident from the above presented results, the proposed concurrent virtual inertia control outcomes better results than other combination of techniques. The presented control scheme performance is also evaluated with PID controller

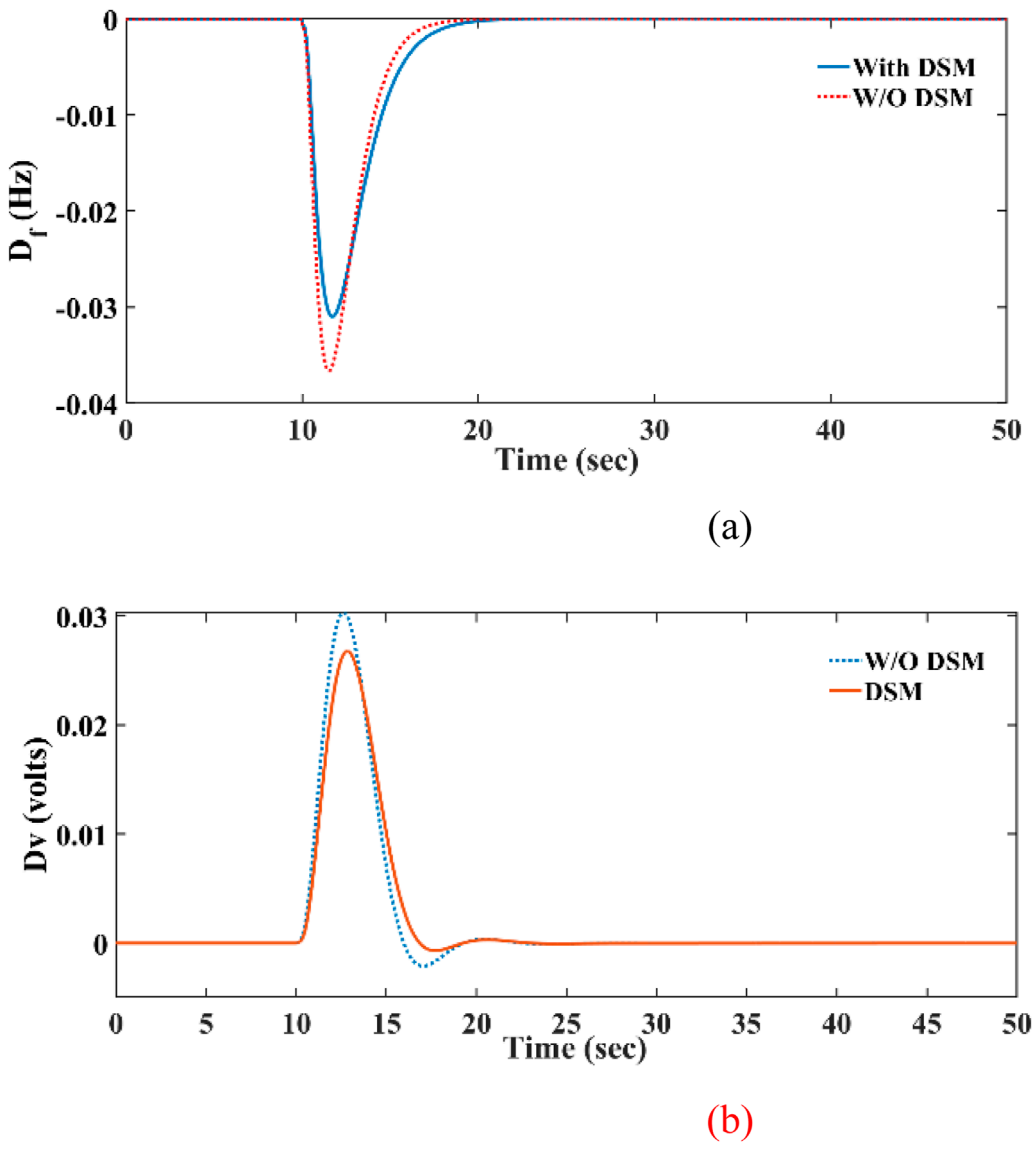

FIGURE 12
Comparison of DSM performance for **(A)** frequency, and **(B)** voltage control.

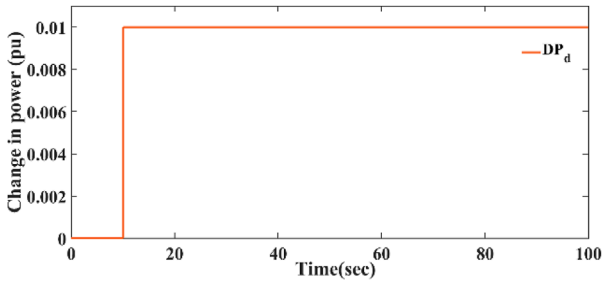

FIGURE 13
Step change in load.

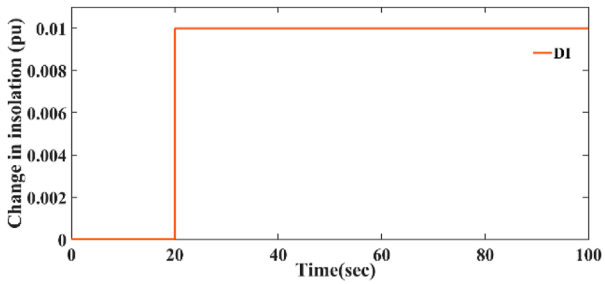

FIGURE 14
Step change in solar insolation.

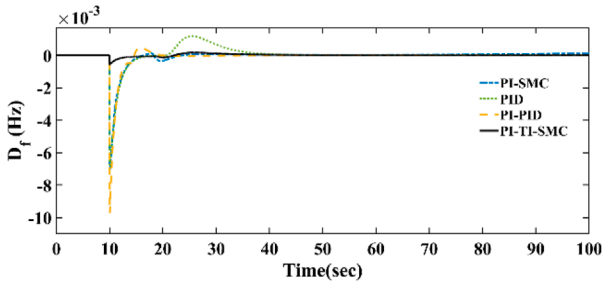

FIGURE 15
Comparison of frequency deviation of controllers.

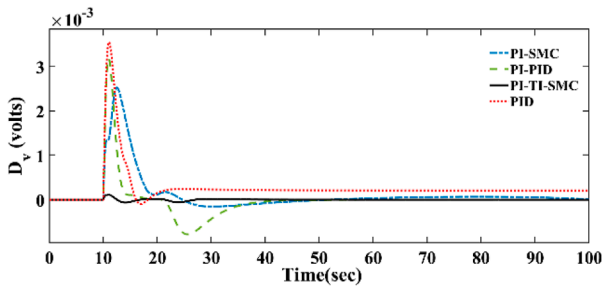

FIGURE 16
Comparison of voltage deviation of controllers.

TABLE 2 Comparison of controllers for step disturbance.

Controllers	DF		DV	
	OS (%)	US (%)	OS (%)	US (%)
PITISMC	0.565	0.595	0.532	1.653
PISMC	0.889	1.858	0.667	1.688
PI-PID	0.93	1.991	1.79	1.891
PID	1.556	3.33	1.955	1.967

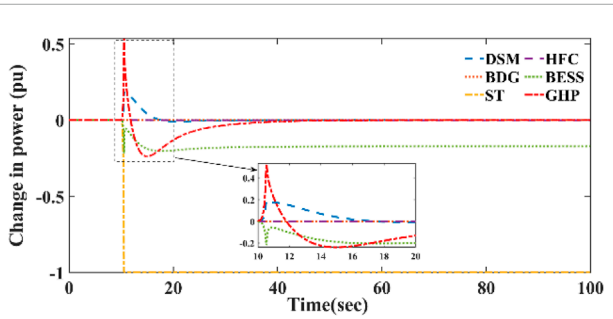

FIGURE 17
Change in active power contribution for step disturbance.

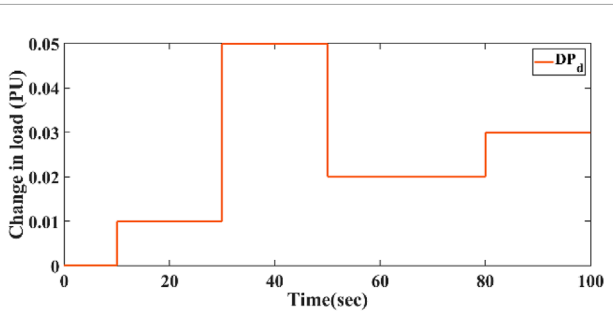

FIGURE 18
Variable change in load.

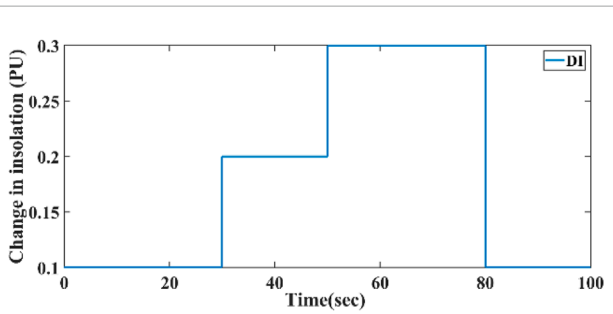

FIGURE 19
Variable change in solar insolation.

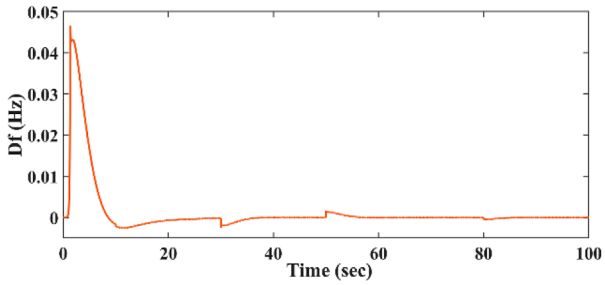

FIGURE 20
Frequency deviation of IHPS for variable disturbance.

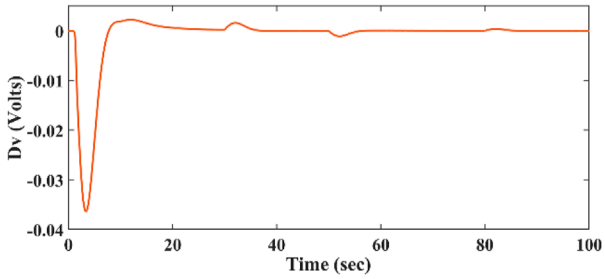

FIGURE 21
Voltage deviation of IHPS for variable disturbance.

TABLE 3 Comparison of controllers for variable disturbance.

Controllers	DF		DV	
	OS (%)	US (%)	OS (%)	US (%)
PITISMC	0.564	0.633	0.778	0.66
PISMC	0.889	2.583	1.937	0.926
PI-PID	1.511	3.33	1.955	1.588
PID	1.938	6.617	1.976	1.967

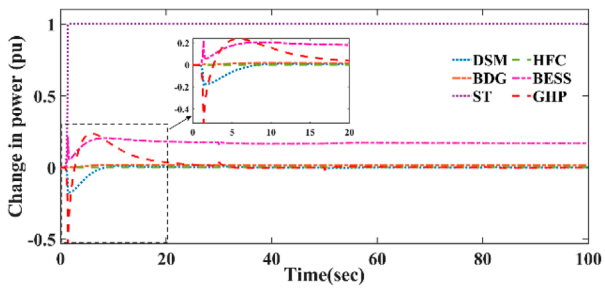

FIGURE 22
Change in active power contribution for variable disturbance.

for frequency and voltage control of IHPS and presented in Figure 11.

4.3 Demand side management:

As stated previously DSM is more precisely implementing technique for frequency and voltage disturbance reduction. In the present work an HEV is considered and its performance in IHPS has been compared as presented in Figure 12.

It is evident from the above results, that providing load side control for concurrent voltage and frequency control by proper DSM technique enhances its stability.

4.4 Selection of controller

The proposed cascaded PI-TISMC is compared with PID, cascaded PI-PID, and PISMC controllers for step disturbance for load and solar insolation as provided in Figures 13, 14.

From results Figures 15, 16 and Table 2 it is clear that the proposed controllers performs better than other controllers for step disturbance. Figure 17 depicts the active power variations of sources in IHPS, due to system disturbances.

4.5 Variable load and insolation

From the above results it identified that TDO optimized cascaded PI-TISMC provides better control of IHPS against frequency and voltage deviations. Now it's been tested for variable load and solar insolation as shown in Figure 18, 19, for the best combination obtained.

From the results provided in Figures 20, 21, proposed technique is effective even for variable disturbances in IHPS and are in permissible range. The superiority among the controllers for variable load disturbance is also supported by Table 3. Figure 22 depicts the active power variations of sources in IHPS, due to variable system disturbances.

5 Conclusion

This paper efficiently established the superiority of the proposed multi energy inertia support for combined voltage and frequency control. The proposed concurrent virtual inertia techniques mitigate the oscillations in better time with an improvement of 2.33 s. Coordinated control mechanism of operating energy storage sources are well executed by developed cascaded PI-TISMC controller that ensures stability of the system to an overall improvement of 6.5% and 7.5% improvement in terms of overshoot and undershoot of disturbance waveforms. With a maiden attempt of comparing unlike classes of optimization techniques for the current work, suggests that the TDO optimized PI-TISMC controller given better results compared to other classes of optimization algorithms. Hence,

the combination exhibits superior performance in minimizing frequency and voltage oscillations in IHPS due to variations in loading and solar insolation.

Data availability statement

The original contributions presented in the study are included in the article/supplementary material, further inquiries can be directed to the corresponding authors.

Author contributions

KK: Methodology, Software, Validation, Writing–original draft. DD: Investigation, Methodology, Writing–review and editing. NS: Formal Analysis, Investigation, Methodology, Writing–original draft. AV: Methodology, Project administration, Software, Writing–original draft. AF: Methodology, Software, Validation, Writing–original draft. AA: Investigation, Methodology, Project administration, Writing–original draft. RU: Data curation, Formal Analysis, Investigation, Writing–original draft.

Funding

The author(s) declare financial support was received for the research, authorship, and/or publication of this article. Researchers Supporting project Number (RSP2024R258), King Saud University, Riyadh, Saudi Arabia.

Conflict of interest

The authors declare that the research was conducted in the absence of any commercial or financial relationships that could be construed as a potential conflict of interest.

Publisher's note

References

Ahmadi, S. A. (2017). Human behavior-based optimization: a novel metaheuristic approach to solve complex optimization problems. *Neural Comput. Appl.* 28, 233–244. doi:10.1007/s00521-016-2334-4

Berrada, A., Loudiyi, K., and Garde, R. (2017). Dynamic modeling of gravity energy storage coupled with a PV energy plant. *Energy* 134, 323–335. doi:10.1016/j.energy.2017.06.029

Bhuyan, M., Barik, A. K., and Das, D. C. (2023). Chaotic butterfly optimization algorithm based cascaded PI-TID controller for frequency control in three area hybrid microgrid system. *Optim. Control Appl. Meth* 44, 2595–2619. doi:10.1002/oca.2994

Bhuyan, M., Kumar Barik, A., and Chandra Das, D. (2019). A Comparative analysis of DSM based autonomous hybrid microgrid using PSO and SCA. *Proc. 2019 IEEE Symposium (TENSYMP)* 27, 765–770. doi:10.1109/tensymp46218.2019.8971155

Chandra Sahu, P., Jena, S., Mohapatra, S., and Debdas, S. (2023). Impact of energy storage devices on microgrid frequency performance: a robust DQN based grade-2 fuzzy cascaded controller. *e-Prime - Adv. Electr. Eng. Electron. Energy* 6, 100288. doi:10.1016/j.prime.2023.100288

Chandra Sahu, P., and Ranjan Samantaray, S. (2023). Resilient frequency stability of a PV/wind penetrated complex power system with CSA tuned robust Type-2 fuzzy cascade PIF Controller. *Electr. Power Syst. Res.* 225, 109815. doi:10.1016/j.epsr.2023.109815

Das, A., and Roy, P. (2016). Improved performance of cascaded fractional- order SMC over cascaded SMC for position control of a ball and plate system. *IETE J. Res.* 63, 238–247. doi:10.1080/03772063.2016.1258336

Das, D. C., Roy, A. K., and Sinha, N. (2011). PSO based frequency controller for wind- solar-diesel hybrid energy generation/energy storage system. *Int. Conf. Energy, Automation, Signal*. doi:10.1109/ICEAS.2011.6147150

Das, D.Ch, Roy, A. K., and Sinha, N. (2012). GA based frequency controller for solar thermal-diesel-wind hybrid energy generation_energy storage system. *Electr. Power Energy Syst.* 43, 262–279. doi:10.1016/j.ijepes.2012.05.025

Dehghani, M., Hubalovsky, S., and &Trojovsky, P. (2022). Tasmanian devil optimization: a new bio-inspired optimization algorithm for solving optimization algorithm. *IEEE Access* 10, 19599–19620. doi:10.1109/ACCESS.2022.3151641

Denholm, P., Mai, T., Kenyon, R. W., Kroposki, B., and O'malley, M. (2020). Inertia and the power grid: a guide without the spin. Available at: www.nrel.gov/publications.

Ghosh, A., Singh, O., Ray, A. K., and Jamshidi, M. (2021). A gravitational search algorithm-based controller for multiarea power systems: conventional and renewable sources with variable load disturbances and perturbed system parameters. *IEEE Syst. Man, Cybern. Mag.* 7 (3), 20–38. doi:10.1109/msmc.2021.3066149

Guha, Di., Roy, P. K., and Banerjee, S. (2021). Fractional-order sliding mode controller applied for load frequency control of power system. *2021 IEEE 4th Int. Conf. Comput. Power Commun. Technol. GUCON 2021* 173, 1–7. doi:10.1109/GUCON50781.2021.9573621

Jiao, N., Wang, S., Ma, J., Liu, T., and Zhou, D. (2024). Sideband harmonic suppression analysis based on vector diagrams for CHB inverters under unbalanced operation. *IEEE Trans. Industrial Electron.* 71 (1), 427–437. doi:10.1109/TIE.2023.3247797

Ju, Y., Liu, W., Zhang, Z., and Zhang, R. (2022). Distributed three-phase power flow for AC/DC hybrid networked microgrids considering converter limiting constraints. *IEEE Trans. Smart Grid* 13 (3), 1691–1708. doi:10.1109/TSG.2022.3140212

Khan, I. A., Mokhlis, H., Mansor, N. N., Illias, H. A., Awalin, L. J., and Wang, Li (2023). New trends and future directions in load frequency control and flexible power system: a comprehensive review. *Alexandria Eng. J.* 71, 263–308. doi:10.1016/j.aej.2023.03.040

Kumar, A., Anwar, M. N., and Kumar, S. (2021). Sliding mode controller design for frequency regulation in an interconnected power system. *Prot. Control Mod. Power Syst.* 6 (1), 6. doi:10.1186/s41601-021-00183-1

Kumar Barik, A., Chandra Das, D., Rasanandamuduli, (2019). Demand response supported optimal load- frequency regulation of sustainable energy based four-interconnected unequal hybrid microgrids. *ICSETS-2019* 75, 273–278. doi:10.1109/icsets.2019.8745069

Kumar Barik, A., and Das, D. C. (2019). Proficient load-frequency regulation of demand response supported bio-renewable cogeneration based hybrid microgrids with quasi-oppositional selfish-herd optimisation. *IET generation Transm. distribution* 13, 2889–2898. doi:10.1049/iet-gtd.2019.0166

Kumar Mohapatra, A., Mohapatra, S., Pattnaik, A., and Chandra Sahu, P. (2024). Design and modelling of an AI governed type-2 Fuzzy tilt control strategy for AGC of a multi-source power grid in constraint to optimal dispatch. *Electron. Energy* 7, 100487. doi:10.1016/j.prime.2024.100487

Latif, A., Suhail Hussain, S. M., Iqbal, A., Chandra Das, D., Ustun, T. S., and Ahmed, A.-D. (2023). Concurrent frequency–voltage stabilization for hybrid microgrid with virtual inertia support. *IET Renew. power Gener.* 17, 2257–2275. doi:10.1049/rpg2.12729

Li, S., Zhao, X., Liang, W., Hossain, M. T., and Zhang, Z. (2022). A fast and accurate calculation method of line breaking power flow based on taylor expansion. *Front. Energy Res.* 10. doi:10.3389/fenrg.2022.943946

Liu, Z., Cheng, X., Peng, X., Wang, P., Zhao, X., Liu, J., et al. (2024). A review of common-mode voltage suppression methods in wind power generation. *Renew. Sustain. Energy Rev.* 203, 114773. doi:10.1016/j.rser.2024.114773

Ma, K., Yu, Y., Yang, B., and Yang, J. (2019). Demand-side energy management considering price oscillations for residential building heating and ventilation systems. *IEEE Trans. Industrial Inf.* 15 (8), 4742–4752. doi:10.1109/TII.2019.2901306

Meng, Q., Hussain, S., Luo, F., Wang, Z., and Jin, X. (2024a). An online reinforcement learning-based energy management strategy for microgrids with centralized control. *IEEE Trans. Industry Appl.*, 1–10. doi:10.1109/TIA.2024.3430264

Meng, Q., Tong, X., Hussain, S., Luo, F., Zhou, F., Liu, L., et al. (2024b). Revolutionizing photovoltaic consumption and electric vehicle charging: a novel approach for residential distribution systems. *IET Generation, Transm. and Distribution* 18, 2822–2833. doi:10.1049/gtd2.13232

Mi, Y., Fu, Y., Wang, C., and Wang, P. (2013). Decentralized sliding mode load frequency control for multi-area power systems. *IEEE Trans. Power Syst.* 28 (4), 4301–4309. doi:10.1109/TPWRS.2013.2277131

Miao, C., Wang, Q., and Tang, Y. (2023a). A multi-energy inertia-based power support strategy with gas network constraints. *Prot. Control Mod. Power Syst.* 8 (1), 18. doi:10.1186/s41601-023-00292-z

Miao, C., Wang, Q., and Tang, Y. (2023b). A gas-thermal inertia-based frequency response strategy considering the suppression of a second frequency dip in an integrated energy system. *Energy* 263, 125880. doi:10.1016/j.energy.2022.125880

Pavan Kumar, K. K., Chandra Das, D., Soren, N., and Chandra Sahoo, S. (2024). Tilt integral sliding mode control approach for real-time parameter variation-based frequency control of hybrid power system using improved african vulture optimization. *Arabian J. Sci. Eng.* 49, 15849–15862. doi:10.1007/s13369-023-08631-w

Ranjan, S., Latif, A., Das, D. C., Sinha, N., Hussain, S. M. S., Ustun, T. S., et al. (2021). Simultaneous analysis of frequency and voltage control of the interconnected hybrid power system in presence of FACTS devices and demand response scheme. *Energy Rep.* 7, 7445–7459. doi:10.1016/j.egyr.2021.10.100

Report on Assessment of Inertia in Indian Power System (2022). *Power system operation corporation limited in collaboration with Indian Institute of Technology*. Bombay.

Roy, P., Das, A., and Roy, B. K. (2018). Cascaded fractional order sliding mode control for trajectory control of a ball and plate system. *Trans. Inst. Meas. Control* 40, 701–711. doi:10.1177/0142331216663826

Shirkhani, M., Tavoosi, J., Danyali, S., Sarvenoee, A. K., Abdali, A., Mohammadzadeh, A., et al. (2023). A review on microgrid decentralized energy/voltage control structures and methods. *Energy Rep.* 10, 368–380. doi:10.1016/j.egyr.2023.06.022

Tamrakar, U., Shrestha, D., Maharjan, M., Bhattarai, B. P., Hansen, T. M., and &Tonkoski, R. (2017). Virtual inertia: current trends and future directions. *Appl. Sci. (Basel).* 7, 654. doi:10.3390/app7070654

Tian, H., Zhao, M., Liu, J., Wang, Q., Yu, X., and Wang, Z. (2024). Dynamic analysis and sliding mode synchronization control of chaotic systems with conditional symmetric fractional-order memristors. *Fractal Fract.* 8 (6), 307. doi:10.3390/fractalfract8060307

Vrdoljak, K., Peric, N., and Petrovic, I. (2009). Sliding mode based load-frequency control in power systems. *Electr. power Syst. Res.* 80 (5), 514–527. doi:10.1016/j.epsr.2009.10.026

Wang, H., Sun, W., Jiang, D., and Qu, R. (2023). A MTPA and flux-weakening curve identification method based on physics-informed network without calibration. *IEEE Trans. Power Electron.* 38 (10), 12370–12375. doi:10.1109/TPEL.2023.3295913

Wang, R., Gu, Q., Lu, S., Tian, J., Yin, Z., Yin, L., et al. (2024). FI-NPI: exploring optimal control in parallel platform systems. *Electronics* 13 (7), 1168. doi:10.3390/electronics13071168

Xinxin, L. V., Sun, Y., Hu, W., and dinavahi, V. (2020). Robust load frequency control for networked power system with renewable energy via fractional-order global sliding mode control. *IET Renew. power Gener.* 15 (5), 1046–1057. doi:10.1049/rpg2.12088

Yaghoubi, E., Yaghoubi, E., Khamees, A., Razmi, D., and Lu, T. (2024). A systematic review and meta-analysis of machine learning, deep learning, and ensemble learning approaches in predicting EV charging behavior. *Eng. Appl. Artif. Intell.* 135, 108789. doi:10.1016/j.engappai.2024.108789

Yang, M. S., and Lu, H. C. (1999). Sliding mode load-frequency controller design for dynamic stability enhancement of large-scale interconnected power systems. *IEEE Int. Symposium Industrial Electron.* 3, 1316–1321. doi:10.1109/isie.1999.796894

Zhang, H., Wu, H., Jin, H., and Li, H. (2023). High-dynamic and low-cost sensorless control method of high-speed brushless DC motor. *IEEE Trans. Industrial Inf.* 19 (4), 5576–5584. doi:10.1109/TII.2022.3196358

Zhang, J., Feng, X., Zhou, J., Zang, J., Wang, J., Shi, G., et al. (2023). Series-shunt multiport soft normally open points. *IEEE Trans. Industrial Electron.* 70 (11), 10811–10821. doi:10.1109/TIE.2022.3229375

Zhang, J., Liu, Y., Zhou, J., Zang, J., Shi, G., Wang, J., et al. (2024). A novel multiport transformer-less unified power flow controller. *IEEE Trans. Power Electron.* 39 (4), 4278–4290. doi:10.1109/TPEL.2023.3347900

Zhou, B., Huang, X., Lin, C., Zhang, H., Peng, J., Nie, Z., et al. (2024a). Experimental study of a WEC array-floating breakwater hybrid system in multiple-degree-of-freedom motion. *Appl. Energy* 371, 123694. doi:10.1016/j.apenergy.2024.123694

Zhou, B., Lin, C., Huang, X., Zhang, H., Zhao, W., Zhu, S., et al. (2024b). Experimental study on the hydrodynamic performance of a multi-DOF WEC-type floating breakwater. *Renew. Sustain. Energy Rev.* 202, 114694. doi:10.1016/j.rser.2024.114694

Zhu, Z., Ye, C., and Wu, S. (2021). Comprehensive control method of energy storage system to participate in primary frequency regulation with adaptive state of charge recovery. *Int. Trans. Electr. Energy Syst.* 31 (12). doi:10.1002/2050-7038.13220

10.3389/fenrg.2024.1466165

Nomenclature

AVOA	African Vulture Optimization Algorithm
AVR	Automatic Voltage Control
BDGS	Bio-Diesel Generator System
BESS	Battery Energy Storage System
CBOA	Chaotic Butterfly Optimization Algorithm
DSM	Demand Side Management
ESS	Energy Storage Sources
FACTS	Flexible Ac Transmission Systems
FC	Fuel Cell
FOSMC	Fractional Order Smc
GA	Genetic Algorithm
GHPS	Gravity Hydro Energy Storage System
GSA	Gravitational Search Algorithm
HBBO	Human Behaviour-Based Optimization
HEV	Hybrid Electric Vehicle
IES	Integrated Energy Systems
IHPS	Isolated Hybrid Power System
IOPID	Integer Order Proportional-Integral-Derivative
ISE	Integral Square Error
LFC	Load Frequency Control
NREL	National Renewable Energy Laboratory
PEMFC	Photon Exchange Membrane Fuel Cell
PFR	Primary Frequency Response
PID	Proportional Integral Derivative
PI-TISMC	Proportional Integral and Tilt Integral SMC
TID	Tilt Integral Derivative
TDO	Tasmanian Devil Optimization
$\Delta P_{bg}, \Delta X_{bg}$	Output states of inlet valve and engine of BDEG
$\Delta P_s, \Delta T_p, \Delta P_m, \Delta X_c, \Delta T_h, \Delta P_{sc}$	Output states of steam chamber, pressure control, temperature control and thermal storage of ST
$\Delta P_g, \Delta X_{gh}, \Delta X_{ga'}$	Output states of aqua electrolyzer and hydrogen storage of FC
Δf	Frequency deviation
Δv	Voltage deviation
ΔP_T	Total output power deviation of power system
ΔP_{ST}	Total output power deviation of solar thermal system
ΔP_{FC}	Total output power deviation of fuel cell
ΔP_{BDEG}	Total output power deviation of bio-diesel generation system
ΔP_{BESS}	Total output power deviation of battery energy storage system
ΔP_{GHPS}	Total output power deviation of gravity hydro energy storage system
ΔP_{HEV}	Total output power deviation of hybrid electric vehicle system
ΔP_{L1}	Step change in load
$K_{be}, K_{ba}, T_{be}, T_{ba}$	Gain and time constants of BDEG
ΔP_D	Output of virtual damping control (VD)
ΔP_{DP}	Output of virtual droop control (VDP)
ΔP_{I1}	Output of virtual inertia control (VI)
ΔP_{I2}	Output of virtual negative inertia control (VNI)
K_D, K_I, K'_I	Proportional constants of VD, VI, and VNI.
ΔP_{HEV}	Total output power deviation of HEV
Δf_m	Max allowable limit of frequency deviation supported by HEV
ΔP_{DSM}	Total output power deviation of DSM
K_{HEV}, T_{HEV}	Gain and time constants of HEV
ΔP_{SOC}	State of charge of HEV
PSO	Particle Swarm Optimization
RES	Renewable Energy Sources
SMC	Sliding Mode Control
ST	Settling time
OS	Overshoot
US	Undershoot
$\Delta P_{b'}$	Output states of BESS
$\Delta P_h, \Delta X_{gc}, \Delta X_{gg'}$	Output states of governer, TDC and hydraulic turbine of GHPS
$\Delta X_f, \Delta X_e, \Delta X_a, \Delta X_s, \Delta \delta_2$	output states of generator field, exciter, amplifier of voltage control